Silicon Synaptic Adaptation Mechanisms for Homeostasis and Contrast Gain Control

Shih-Chii Liu, *Member, IEEE,* and Bradley A. Minch, *Member, IEEE*

Abstract—In this paper, we explore homeostasis in a silicon integrate-and-fire neuron. The neuron adapts its firing rate over time periods on the order of seconds or minutes so that it returns to its spontaneous firing rate after a sustained perturbation. Homeostasis is implemented via two schemes. One scheme looks at the presynaptic activity and adapts the synaptic weight depending on the presynaptic spiking rate. The second scheme adapts the synaptic "threshold" depending on the neuron's activity. The threshold is lowered if the neuron's activity decreases over a long time and is increased for prolonged increase in postsynaptic activity. The presynaptic adaptation mechanism modoolsels the contrast adaptation responses observed in simple cortical cells. To obtain the long adaptation timescales we require, we used floating-gates. Otherwise, the capacitors we would have to use would be of such a size that we could not integrate them and so we could not incorporate such long-time adaptation mechanisms into a very large-scale integration (VLSI) network of neurons. The circuits for the adaptation mechanisms have been implemented in a 2-μm double-poly CMOS process with a bipolar option. The results shown here are measured from a chip fabricated in this process.

Index Terms—Adaptation, contrast gain control, floating-gate circuits, homeostasis, integrate-and-fire neurons, long time constants, neuron circuits.

I. INTRODUCTION

RESEARCHERS have postulated continual adaptation mechanisms, which, for example, preserve the firing rate of the neuron over long time invervals [2] or use the presynaptic spiking statistics to adapt the spiking rate of the neuron so that the distribution of this spiking rate is uniformly distributed [3]. This homeostatic process (or homeostasis) whereby a neuron returns to a stable state of equilibrium after a long-term perturbation, is observed in *in vitro* recordings [4]. In these recordings, the cell returns to its original spiking rate in a couple of days if the potassium or sodium conductances of the cell are perturbed by adding antagonists. These adaptation mechanisms are important in preserving the sensitivity of the neuron to changes in input activity.

This paper differs from previous work that explores the adaptation of the neuron's firing threshold and gain through the regulation of Hodgkin–Huxley-like conductances [5] and regulation of a silicon Morris–Lecar neuron to perturbation in

S.-C. Liu is with the Institute for Neuroinformatics, University of Zurich and ETH Zurich, CH-8057 Zurich, Switzerland (e-mail: shih@ini.phys.ethz.ch).

B. A. Minch is with the School of Electrical and Computer Engineering, Cornell University, Ithaca, NY 14853-5401 USA (e-mail: minch@ee.cornell.edu).

the conductances [6]. These mechanisms do not use long-time constant adaptation mechanisms in regulating the output of the neuron. Our neuron circuit is a simple integrate-and-fire neuron (we do not model details of the Hodgkin–Huxley conductances) and our adaptation mechanisms have time constants of seconds to minutes. These long time constants are important in a system that has to perform in a noncontrolled environment. This homeostatic process allows the system to change its equilibrium state and to maintain a high dynamic range by adapting out slow changes in the environment.

In this work, we show two different synaptic circuits: One circuit adapts its synaptic weight to changes in the presynaptic spiking rates, and the other circuit implements postsynaptic adaption. The presynaptic adaptation mechanism can describe the contrast gain control curves measured in cortical simple cells [7]. These circuits were fabricated on a 2-μm double-poly CMOS process with a bipolar option. To implement the long time constant circuits, we used floating gates instead of capacitors. The floating gate is not connected to any diffusion nodes so the charge on this gate cannot leak to the substrate. Tunneling and injection mechanisms are used to remove charge from and to add charge onto a floating gate, respectively, [8]. A simple model of these mechanisms has been described elsewhere [9]. Even though the injection mechanism that we employed in this work made use of the special bipolar option in the CMOS process in which we fabricated the circuits, the circuits can be altered easily for any digital CMOS process by instead using pFET hot-electron injection [10]. We incorporated these synaptic mechanisms into a simple integrate-and-fire neuron circuit [11].

II. ADAPTATION MECHANISMS IN SILICON NEURON CIRCUIT

In order to permit continuous operation with only positive polarity bias voltages, we use two distinct mechanisms to modify the floating-gate charges in our neuron circuits: electron tunneling and hot-electron injection. We use Fowler–Nordheim tunneling through high-quality gate oxide to remove electrons from the floating gates [12]. Here, we apply a large voltage across the oxide, which reduces the width of the Si–SiO$_2$ energy barrier to such an extent that electrons are likely to tunnel through the barrier. We model the tunneling current with a simplified model of the Fowler–Nordheim tunneling [12] given by

$$I_{\text{tun}} = I_{ot} e^{-(V_o/V_{\text{ox}})} \tag{1}$$

where $V_{\text{ox}} = V_{\text{tun}} - V_{fg}$ is the voltage across the tunneling oxide; V_{tun} is the tunneling voltage; V_{fg} is the voltage of the
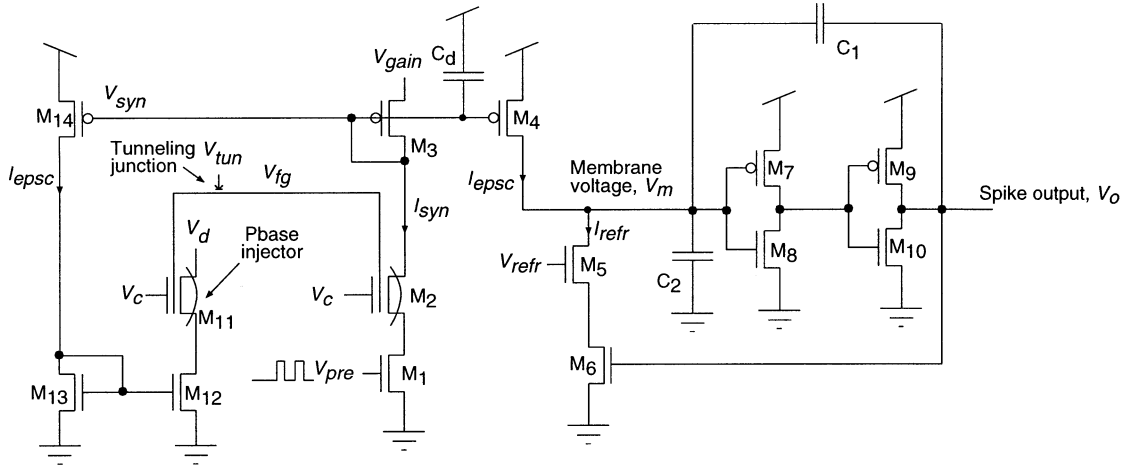
Fig. 1.   Schematic of an integrate-and-fire neuron circuit with a presynaptic long-time-constant adaptation mechanism. The neuron circuit comprises transistors M_5 to M_{10} and capacitors C_1 and C_2. The operation of the circuit is described in the text. The current I_{epsc} that charges up the membrane voltage V_m is generated by the synaptic circuit comprising of transistors M_1 to M_4 and capacitor C_d. The source voltage, V_{gain}, of M_3 and C_d determine the dynamics and current gain of the synaptic circuit. The presynaptic spike input, V_{pre}, goes to the gate of M_1 and the synaptic efficacy is set by the gate voltage V_{fg} of the pbase transistor M_2. The voltage V_{fg} of the floating gate can be increased by turning on the tunneling mechanism and decreased by turning on the injection mechanism. The tunneling mechanism is continuously on and the tunneling rate is set by V_{tun}. The injection mechanism is enabled through the second pbase transistor M_{11} by setting V_d to a high voltage. In our experiments, V_d was set to 4 V during injection. The amount of injection is determined by the current through M_{11} and its drain-to-channel voltage. The current through M_{11} mirrors that of I_{epsc} through transistors M_3, M_4 and M_{12} to M_{14}. The voltage V_{fg} can be influenced through the voltage V_c to the top gate of transistors M_2 and M_{11}. This voltage was kept constant during the experiments described in the text.

floating gate; and I_{ot} and V_o are measurable device parameters. For the 400-Å oxides that are typical of a 2-μm CMOS process, a typical value of V_o is 1000 V and an oxide voltage of about 30 V is required to obtain an appreciable tunneling current. Note that, in more modern technologies with thinner gate oxides, the oxide voltage required to get significant tunneling becomes much smaller.

We use subthreshold channel hot-electron injection in an nFET [8] to add electrons to the floating gate. In this process, electrons in the channel of the nFET accelerate in the high electric field that exists in the depletion region near the drain, gaining enough energy to surmount the Si–SiO$_2$ energy barrier (about 3.2 eV). To facilitate the hot-electron injection process, we locally increase the substrate doping density of the nFET using the p-base layer that is normally used to form the base of a vertical npn bipolar transistor. The symbol for this transistor structure is denoted by M_2 in Fig. 1. The p-base substrate implant simultaneously increases the electric field at the drain end of the channel and increases the nFETs threshold voltage from 0.8 V to about 6 V, permitting subthreshold operation at gate voltages that permit the collection of the injected electrons by the floating gate. We model the hot-electron injection current with a simplified injection model [10] given by

$$I_{inj} = \eta I_s e^{\phi_{dc}/V_{inj}} \qquad (2)$$

where I_s is the source current; ϕ_{dc} is the drain-to-channel voltage; and η and V_{inj} are measurable device parameters. The value of V_{inj} is a bias dependent injection parameter and typically ranges from 60 mV to 0.1 V. This circuit can easily be changed so that we make use of pFET hot-electron injection in a standard CMOS process [10].

III. PRESYNAPTIC ADAPTATION

The presynaptic mechanism adapts the synaptic efficacy to the presynaptic firing rate over long time constants. The circuit for this adaptation mechanism is shown in Fig. 1. The neuron circuit comprises M_5 to M_{10}, and the capacitors C_1 and C_2 [11]. The current I_{epsc} charges up the membrane voltage of the neuron V_m until it exceeds a threshold. The spike output of the neuron V_o then becomes active and starts discharging V_m through M_5 and M_6. The capacitor C_1 provides positive feedback because the change in V_o is coupled back into V_m. The amount of coupling is given by $(C_1/(C_1 + C_2))V_o$. The refractory current I_{refr} discharges V_m when V_o is active. Once V_m is discharged past the transition threshold of the inverter, V_o becomes inactive and the cycle of charging and discharging starts again. The voltage, V_{refr}, controls the rate at which the neuron is discharged; thus the refractory period and pulse width of the spike output V_o. The period of the spike is $T = C_1(V_{dd}/I_{epsc}) + C_1(V_{dd}/(I_{refr} - I_{epsc}))$, where V_{dd} is the power supply to the chip. The spiking rate of the neuron, f_o is approximately

$$f_o = m I_{epsc} \qquad (3)$$

for large I_{refr}. In this equation, $m = 1/C_1 V_{dd}$.

The current I_{syn} is generated by a series connection of two transistors; M_1, which is driven by the presynaptic spike input, V_{pre}, and M_2, which is driven by the floating-gate voltage, V_{fg}. The floating-gate voltage controls the efficacy of the synapse. A discrete amount of charge is removed from the capacitor, C_d, during a presynaptic spike. The charge removed depends on the pulse width, T_δ, of the spike and V_{fg} [13]. The current I_{syn} is mirrored through transistors, M_3 and M_4 into the excitatory postsynaptic current I_{epsc}. The dynamics and gain of the current

mirror, which affects the value of I_{epsc} depend on C_d and V_{gain}. Assuming that the transistors are operating in subthreshold, the steady-state current for a presynaptic frequency f_i, is given by

$$I_{\text{epsc}} = \left(e^{(I_{opb}e^{\kappa V_{fg0}/U_T}T_\delta)/Q_T} - 1 \right) A Q_T f_i \qquad (4)$$

where $A = e^{(V_{dd}-V_{gain})/U_T}$; $Q_T = C_d U_T / \kappa$ is the thermal charge stored on the capacitor C_d; U_T is the thermal voltage; κ is the coupling efficiency from the gate to the channel of a subthreshold transistor; I_{opb} is the preexponential constant of the subthreshold current through the pbase transistor; and V_{fg0} is the steady-state voltage of the floating gate. For small $e^{(I_{opb}e^{\kappa V_{fg0}/U_T}T_\delta)/Q_T}$, (4) simplifies to

$$I_{\text{epsc}} = I_{\text{eff}} T_\delta A f_i \qquad (5)$$

where $I_{\text{eff}} = I_{opb}e^{\kappa V_{fg0}/U_T}$.

The tunneling mechanism (controllable through V_{tun}) is continuously on so the efficacy of the synapse increases slowly over time. The injection circuitry consists of the transistors M_{11} to M_{14}. Transistor M_{11} is the injection transistor. By setting the drain voltage V_d of M_{11} at a high enough voltage, injection occurs in this transistor. The injection current depends on the current flowing through M_{11} and its drain-to-channel voltage. The current through M_{11} mirrors that of I_{epsc} through transistors M_3, M_4, and M_{12} to M_{14}. By setting the dimensions of the current-mirror transistors, M_{14} and M_4, to the same values, and the dimensions of M_{12} and M_{13} to the same values, the injection current depends on I_{epsc} through the equation described in (2). To understand the dynamics of this adaptation mechanism, we compute the transfer function of the neuron for both the transient and steady-state conditions in Sections III-A and III-B. We will also show in Section V that this presynaptic adaptation mechanism can lead to the contrast adaptation curves observed in the visual cortex.

A. Steady-State Analysis

To obtain the steady-state spike rate of the neuron in response to a fixed presynaptic input frequency, we need to solve for I_{epsc} the synaptic current to the neuron. This current is determined by V_{fg}. In steady-state, the tunneling current [from (1)]

$$I_{\text{tun}} = I_{ot}e^{-(V_o/(V_{\text{tun}}-V_{fg0}))} \qquad (6)$$

is equal to the injection current defined through (2)

$$I_{\text{inj}} = \eta e^{\phi_{dc}/V_{\text{inj}}} I_{\text{epsc}}$$

and by substituting I_{epsc} from (5), the injection current can be reexpressed as

$$I_{\text{inj}} = \eta e^{\phi_{dc}/V_{\text{inj}}} I_{\text{eff}} A Q_T f_i. \qquad (7)$$

By equating (6) and (7), we solve for the steady-state floating-gate voltage V_{fg0}, and then compute the synaptic efficacy

$$I_{\text{eff}} = I_{opb}e^{\kappa V_{fg0}/U_T} \approx \frac{I_m}{(f_i T_\delta)}. \qquad (8)$$

I_m is assumed to be constant and depends on the preexponential constants of the injection current equation and the tunneling parameters. The steady-state input current is then

$$I_{\text{epsc}} = I_{\text{eff}} T_\delta A f_i \approx I_m A \qquad (9)$$

and is approximately independent of the presynaptic input frequency. Hence, the dc gain is zero. This input independence arises because the steady-state synaptic efficacy is inversely proportional to the steady-state presynaptic frequency f_i.

B. Transient Analysis

From (3) and (5), we first express the neuron's spike frequency f_o in terms of presynaptic input frequency f_i

$$f_o = m I_{\text{epsc}} = m I_{\text{eff}} T_\delta A f_i. \qquad (10)$$

By differentiating (10), we can see that the transient gain df_o/df_i decreases with increasing f_i

$$\frac{df_o}{df_i} = \frac{f_o}{f_i}. \qquad (11)$$

C. Experimental Results

We measured both the transient and steady-state dynamics of this circuit, which was fabricated in the 2-μm CMOS process using four presynaptic frequencies (100 Hz, 150 Hz, 200 Hz, and 250 Hz). In these measurements, the drain of the pbase injection transistor V_d (see Fig. 1) was set at 4 V and the tunneling voltage V_{tun} was set at 35.3 V. For each presynaptic frequency, we presented step increases and decreases in the presynaptic rate of 15 Hz, 30 Hz, 45 Hz, and 60 Hz around that frequency. The instantaneous postsynaptic spike response is plotted along one the four steep curves in Fig. 2. After every measurement, the presynaptic rate was returned to its dc value before the next step change in presynaptic frequency. From Fig. 2, we can see that the dc gain is approximately zero as described by (9), while the transient gain of the curves decreased for higher input spiking rates as described by (11).

The dynamics of the adaptation mechanism for a step decrease in the presynaptic frequency (from 350 to 300 Hz at $t = 0$) can be seen from the measurement of the postsynaptic spiking rate of the neuron plotted in Fig. 3. The system adapts over a time constant of minutes back to the initial output frequency. These data show that the synaptic efficacy adapted to a higher weight value over time. The time constant of the adaptation can be increased by either decreasing the tunneling voltage or the pbase injector's drain voltage V_d.

IV. POSTSYNAPTIC ADAPTATION

In the second mechanism, the neuron's spike rate determines the synaptic "threshold." The schematic of this adaptation circuitry is shown in Fig. 4. The floating-gate pbase transistor, M_1 provides an input to the neuron so that the neuron fires at a quiescent rate. Notice that the output of the neuron is now active low. The tunneling mechanism is continuously on so the floating-gate voltage increases with time resulting in an increase in the neuron's spiking rate. On the other hand, the injection
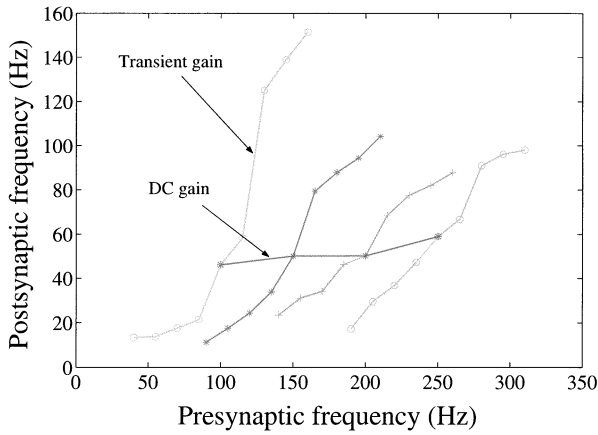
Fig. 2.   Response curves of the neuron in Fig. 1 to different input frequencies when the presynaptic long-time-constant adaptation mechanism is enabled. The transient gain, df_o/df_i of the curves decreases with increasing presynaptic frequencies while the dc gain is approximately zero.
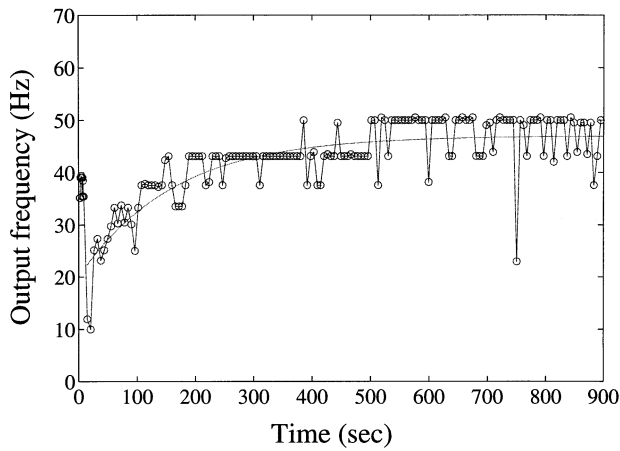

Fig. 3.   Temporal adaptation of postsynaptic spiking rate of the neuron in response to a step decrease in the presynaptic input from 350 Hz to 300 Hz. The smooth line is an exponential fit to the measured data.

mechanism only turns on when the neuron spikes. The time constant of this adaptation can be set for seconds to minutes. The increase in the floating-gate voltage is equivalent to a decrease in the synaptic threshold. If the neuron's activity is high, the injection mechanism turns on thus decreasing the floating-gate voltage and the input current to the neuron. These two opposing mechanisms ensure that the cell will remain at a constant activity under steady-state conditions.

Another way of looking at this process is that the threshold of the neuron is modulated by its output spiking rate. This threshold continuously decreases; however during every output spike, the threshold increases. A circuit which models the adaptation in the firing rate of pyramidal cells to a persistent stimulus was described in [13]. This adaptation mechanism works on short time scales in the order of milliseconds and does not utilize floating gates. That circuit models the fast K adaptation dynamics of pyramidal cells. Our circuit models the long-time constant homeostatic process described in [4]. In our circuit, the output spiking rate always returns to the same quiescent value: This rate is determined by a balance between the average injection current and the quiescent tunneling current.

Temporal changes in the input signal rather than the signal itself, modulates the tonic input current to the neuron. As in Section III, we compute the transfer function of the neuron for both the transient and steady-state conditions in Sections IV-A and IV-B.

A. Steady-State Analysis

As in the presynaptic steady-state analysis, we solve for the input current, $I_{\rm in}$, hence, the floating-gate voltage by using the fact that in steady-state, the tunneling current, $I_{\rm tun}$ defined by

$$I_{\rm tun} = I_{ot}e^{-(V_o/(V_{\rm tun}-V_{fg0}))} \tag{12}$$

is equal to the average of the injection current

$$I_{\rm inj} = I_{\rm opb}e^{\kappa V_{fg0}/U_T}e^{\phi_{dc}/V_{\rm inj}}(f_o T_\delta) \tag{13}$$

where I_{ot} and $I_{\rm opb}$ are preexponential constants; T_δ is the postsynaptic spike's pulse width; and f_o is the output spike rate.

Using (12) to (13) and assuming that V_o, $V_{\rm tun}$, and U_T are constant, we solve first for V_{fg0}, and then solve for the steady-state input current

$$I_{in0} = I_{\rm opb}e^{\kappa V_{fg0}/U_T} \approx \frac{I_m}{(f_o T_\delta)}$$

where I_m is a constant which depends on the tunneling and injection parameters. Because $I_{\rm tun}$ and $I_{\rm inj}$ are independent of the input voltage, the steady-state floating-gate voltage V_{fg0} and hence the steady-state output frequency f_o always returns to the same value.

B. Transient Analysis

We compute the change in the output frequency f_o when a small step input ΔV is applied to V_{ex} in Fig. 4. This step input is coupled into the floating gate and changes its voltage by $\Delta V(C_{\rm gfg}/(C_{\rm gfg} + C_{\rm fgsub}))$, where $C_{\rm gfg}$ is the coupling capacitance from the top gate to the floating gate and $C_{\rm fgsub}$ is the coupling capacitance from the top gate to the substrate. The input current $I_{\rm in}$ immediately after the step input is:

$$I_{\rm in}(t=0+) = I_{in0}e^{\kappa_{\rm eff}\Delta V/U_T}$$

where $\kappa_{\rm eff} = \kappa(C_{\rm gfg}/(C_{\rm gfg} + C_{\rm fgsub}))$. The corresponding increase in f_o is

$$f_o + df_o = f_oe^{\kappa\Delta V/U_T}.$$

If we assume that the steady-state value of the input V_{ex} codes the natural logarithm of the input firing rate f_i, that is, $V_{ex} = U_T \log(f_i/f_c)$ (where f_c is a constant), then $\Delta V = U_T df_i/f_i$. Using the above relationship, we solve for the change in the output frequency, that is

$$\frac{df_o}{f_o} = e^{\kappa\Delta V/U_T} - 1 \approx \kappa\frac{df_i}{f_i}. \tag{14}$$

Equation (14) shows that the transient change in the spike rate of the neuron is proportional to the contrast in the input spike rate. Over time, the floating-gate voltage adapts back to the steady-
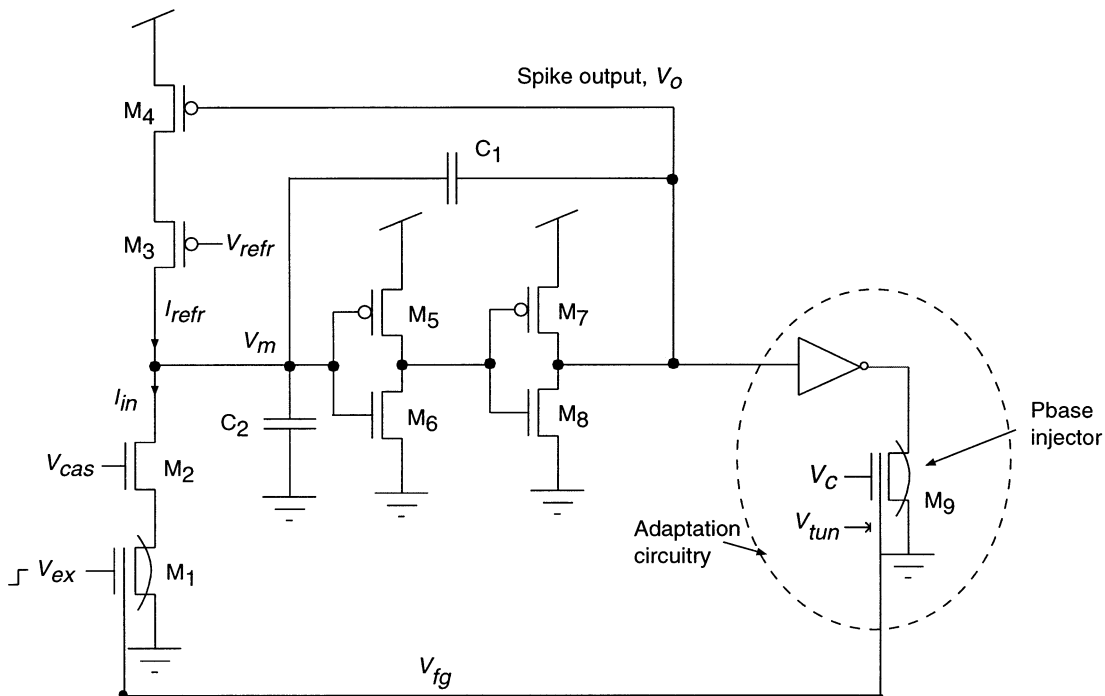
Fig. 4. Schematic of an integrate-and-fire neuron circuit and the postsynaptic long-time-constant adaptation circuit. The neuron circuit consists of transistors M_3 to M_8; and the capacitors, C_1 and C_2. The circuit is similar to the neuron circuit in Fig. 1 except that the input current I_{in} discharges the membrane node and the output V_o is active low. The "threshold" of the synapse is set by the floating-gate voltage, V_{fg}, which drives the pbase transistors M_1. The top gate of M_1 is driven by the presynaptic input V_{ex}. Transistor M_2 is a cascode transistor and constrains the drain voltage of M_1 so that no injection will occur in M_1. The tunneling voltage V_{tun} is set such that there is a low continuous tunneling current. If the neuron does not fire for a while, V_{fg} and, hence, I_{in} will increase until the neuron starts firing. Transistor M_9 acts as the pbase injector. Injection occurs when the drain voltage of M_9 is high, that is, when V_o goes low. The floating-gate voltage can be influenced by the input V_c to the top gate of M_9. Each postsynaptic spike decreases V_{fg} hence increasing the "threshold" of the synaptic transistor M_1.

state condition (due to the continuous tunneling current) and the spiking rate returns to f_o.

C. Experimental Results

In these experiments, V_{tun} was set to 28 V, and the injection voltage was set to 6.6 V. The output frequency of the neuron was measured over a period of 30 min after step voltage decreases of 0.2 V (circles) and 0.3 V (pluses) were applied to V_{ex} (see Fig. 5). The initial spike frequency of about 19 Hz decreased to 13 Hz in response to the step decrease in the input but after this initial perturbation the spiking rate returned to 19 Hz over a period of about 10 min. Similarly, measurements were performed after step increases of 0.2 V and 0.3 V were applied to V_{ex}. In this case, the output frequency of the neuron initially increased to 28 Hz but adapted back to the quiescent rate (20 Hz) over a period of about 10 min.

V. CONTRAST GAIN CONTROL

Presynaptic adaptation dynamics can provide contrast gain control observed in cortical simple cells [7]. Because the gain of the transfer function of the cortical cell for stimulus contrast is high, the output of the neuron is nonsaturating only for a small range of input contrasts. The contrast response function of the neuron shifts when it is presented with a fixed contrast for a long period of time. This shift in the response curves is similar to the shift of the responses of retinal cones to different background intensities. This mechanism increases the dynamic range of the cell. The experiments of [14] show that even the contrast

of a nonpreferred stimulus over 30 s causes adaptation of the neuron's response to stimulus contrast. This observation suggests that the gain control mechanism is presynaptic.

The output firing rate f_{lgn} of the lateral geniculate nucleus (LGN) cells, which are presynaptic to the cortical cell, has an approximately linear dependence on $\log(C)$ (where C is the stimulus contrast) [7]. The firing rate dependence on the contrast can be expressed as

$$f_{\text{lgn}} = \beta \log(C) - \log(\sigma)$$

where $\log(\sigma)$ is the intercept of the curve and β is the gain of the LGN cell. The instantaneous firing rate of the cortical cell f_{ct} to a change in contrast (as described in [7] and shown in Fig. 6) is then

$$f_{ct} = w f_{\text{lgn}} = w(\beta \log(C) - \log(\sigma)) \qquad (15)$$

where w is the synaptic weight. The shifting of the contrast curves can be represented by the dependence of σ on the time-averaged value of C.

Another way of describing the adaptation is by assuming that the weight w adapts to the time-averaged value of f_{lgn} (hence the steady-state stimulus contrast) and σ is constant. Our presynaptic adaptation mechanism gives rise to response curves (Fig. 2) that are similar to the experimental contrast gain curves in [7] (Fig. 6). The input frequency to the neuron circuit in Fig. 1 represents f_{lgn} and w is represented by I_{eff}. As we have seen, the time constant of the weight adaptation mechanism can be set for a time scale of minutes. By adapting the weight of the synapse
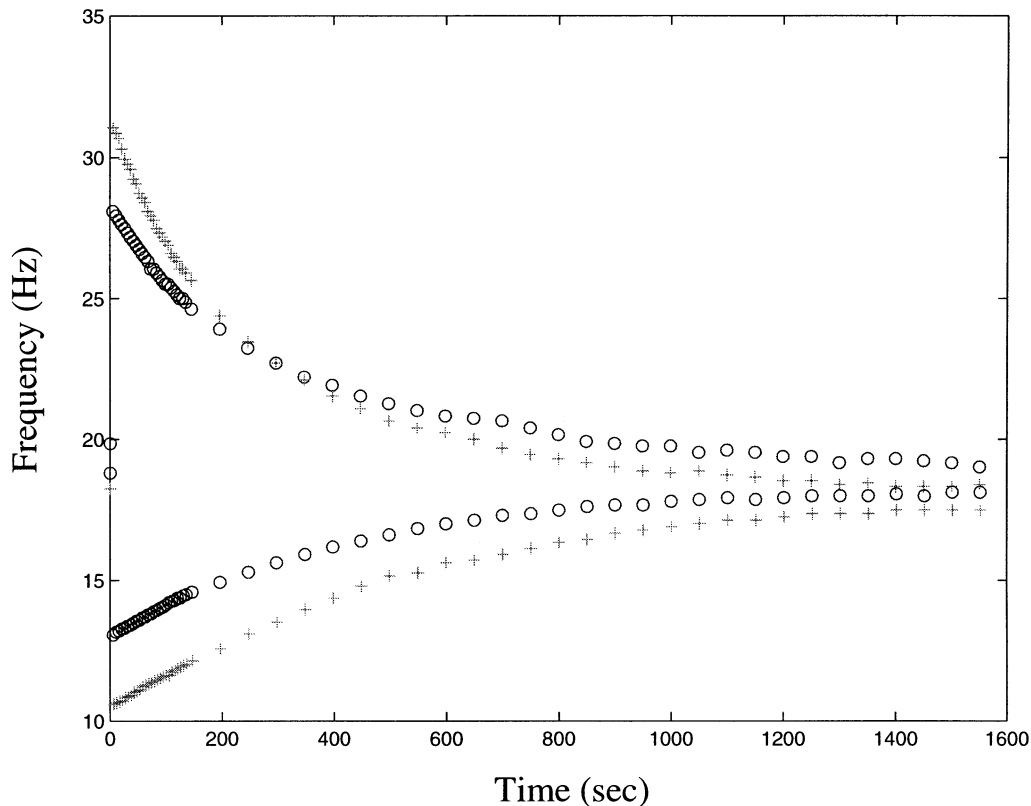
Fig. 5.   Response of the silicon neuron in Fig. 4 to input step increases and decreases of 0.2 V (circles) and 0.3 V (pluses). The adaptation time constant is in the order of about 10 min.
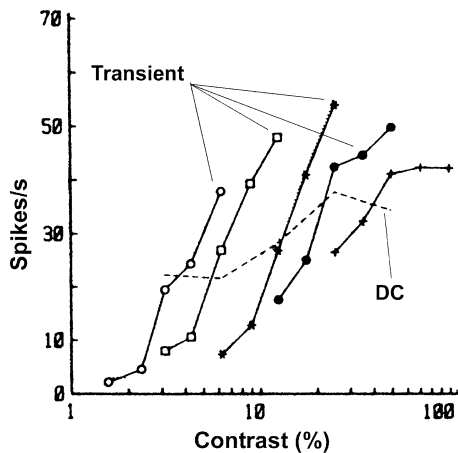

Fig. 6.   Responses of a cortical neuron to drifting grating stimuli as a function of contrast in [7]. The solid curves show the transient gain responses of the neuron around five different adapting contrasts. In this graph, the transient gain decreases for higher adapting contrasts. The dashed curve shows the steady-state response derived from data collected in the last 40 s of an 80 s continuous stimulation at fixed contrasts. Adapted from [7, Fig. 1b] with permission.

to the presynaptic input frequency with a $1/f$ dependence as shown in (8), the steady-state gain of the neuron's contrast response is almost zero while the transient gain decreases with increasing stimulus contrast as seen in (11).

Neurons with depressing synapses [15] where the steady-state excitatory postsynaptic current (EPSC) has a $1/f$ dependence on the presynaptic frequency can implement the presynaptic adaptation process needed to obtain contrast gain control. However, the time constant required for the synapse (as measured

by the EPSC) to reach steady-state is only in the order of hundreds of milliseconds and hence is not of the order of minutes as is observed in the contrast adaptation experiments.

VI. CONCLUSION

In this paper, we show how two long-time constant adaptation mechanisms can be added to a silicon integrate-and-fire neuron in a relatively standard CMOS process. These mechanisms act to maintain homeostasis in the output of the neuron and can be combined with short-time constant depressing or facilitating input synapses [16] to provide a wide range of adapting time constants. These mechanisms increase the neuron's sensitivity to transient changes in the input. The presynaptic adaptation mechanism described here can also account for the contrast gain control mechanism observed in cortical simple cells.

REFERENCES

[1] S.-C. Liu, J. Kramer, G. Indiveri, T. Delbruck, T. Burg, and R. Douglas, "Orientation-selective aVLSI spiking neurons," *Neural Networks (Special Issue on Spiking Neurons in Neuroscience and Technology)*, vol. 14, no. 6/7, pp. 629–643, 2001.
[2] Z. Liu, J. Golowasch, E. Marder, and L. F. Abbott, "A model neuron with activity-dependent conductances regulated by multiple calcium sensors," *J. Neurosci.*, vol. 18, no. 7, pp. 2309–2320, 1998.

[3] M. Stemmler and C. Koch, "How voltage-dependent conductances can adapt to maximize the information encoded by neuronal firing rate," *Nature Neurosci.*, vol. 2, no. 6, pp. 521–527, 1999.

[4] N. S. Desai, L. C. Rutherford, and G. G. Turrigiano, "Plasticity in the intrinsic excitability of cortical pyramidal neurons," *Nature Neurosci.*, vol. 2, no. 6, pp. 515–520, 1999.

[5] J. H. Shin and C. Koch, "Dynamic range and sensitivity adaptation in a silicon spiking neuron," *IEEE Trans. Neural Networks*, vol. 10, pp. 1232–1238, Sept. 1999.

[6] M. F. Simoni and S. P. DeWeerth, "Adaptation in an aVLSI model of a neuron," *IEEE Trans. Circuits Syst. II*, vol. 46, pp. 967–970, July 1999.

[7] I. Ohzawa, G. Sclar, and R. Freeman, "Contrast gain control in the cat visual cortex," *Nature*, vol. 298, no. 5871, pp. 266–268, 1982.

[8] C. Diorio, B. A. Minch, and P. Hasler, "Floating-gate MOS learning systems," in *Proc. Int. Symp. Future Intell. Integrated Electron. (ISFIIE)*, Mar. 14–17, 1999, pp. 515–524.

[9] P. Hasler, "Continuous-time feedback in floating-gate MOS circuits," *IEEE Trans. Circuits Syst. II*, vol. 48, pp. 56–64, Jan. 2001.

[10] P. Hasler, B. A. Minch, and C. Diorio, "Adaptive circuits using pFET floating-gate devices," in *Proc. 20th Anniversary Conf. Advanced Res. VLSI*, D. S. Wills and S. P. DeWeerth, Eds. Atlanta, GA: IEEE Comput. Society Press, 1999, pp. 215–229.

[11] C. Mead, *Analog VLSI and Neural Systems*. Reading, MA: Addison-Wesley, 1989.

[12] M. Lenzlinger and E. H. Snow, "Fowler–Nordheim tunneling into thermally grown SiO_2," *J. Appl. Phys.*, vol. 40, pp. 278–283, 1969.

[13] K. A. Boahen, "The retinomorphic approach: Pixel-parallel adaptive amplification, filtering, and quantization," *Analog Integrated Circuits Signal Processing*, vol. 13, no. 1–2, pp. 53–68, 1997.

[14] B. Ahmed, J. D. Allison, R. J. Douglas, and K. A. Martin, "An intracellular study of the contrast-dependence of neuronal activity in cat visual cortex," *Cerebral Cortex*, vol. 7, pp. 559–570, 1997.

[15] L. F. Abbott, K. Sen, J. A. Varela, and S. B. Nelson, "Synaptic depression and cortical gain control," *Science*, vol. 275, no. 5297, pp. 220–223, 1997.

[16] C. Rasche and R. Hahnloser, "Silicon synaptic depression," *Biol. Cybern.*, vol. 84, no. 1, pp. 57–62, 2001.

Shih-Chii Liu (M'02) received the B.S. degree in electrical engineering from Massachusetts Institute of Technology, Cambridge, in 1983, the M.S. degree in electrical engineering from University of California, Los Angeles, in 1988, and the Ph.D. degree in the Computation and Neural Systems Program from California Institute of Technology, Pasadena, in 1997.

From 1983 to 1985, she was with Gould American Microsystems and from 1985 to 1988, she was with LSI Logic. From 1988 to 1997, she was with Rockwell International Research Labs. She is currently an Ueberassistentin, Institute of Neuroinformatics, University of Zurich/ETH Zurich, Zurich, Switzerland. Her research interests include neuromorphic modeling of vision and cortical processing, networks for behavior generation, and hybrid analog/digital signal processing.

Bradley A. Minch (S'89–M'97) received the B.S. degree in electrical engineering with distinction from Cornell University, Ithaca, NY, in May 1991 and the Ph.D. degree in computation and neural systems from the California Institute of Technology, Pasadena, in June 1997.

He is currently an Assistant Professor in the School of Electrical and Computer Engineering, Cornell University, Ithaca, NY. His research interests include the analog and digital integrated circuit design, translinear circuits, log-domain filters, and adaptive floating-gate MOS circuits.

Dr. Minch received the IEEE Electron Devices Society's Paul Rappaport Award in 1996. He is a Member of Tau Beta Pi, Eta Kappa Nu, and Phi Kappa Phi honor societies.